# Microstructural observation of $ZnAl_2O_4$ formation affected by the physical nature of $Al_2O_3$ in the presence of LiF

MINORU HASHIBA, MINORU SHIGEMITSU, YUKIO NURISHI
*Department of Chemistry, Faculty of Engineering, Gifu University, 1-1, Yanagido, Gifu-shi 501-11, Japan*

Microstructures of $ZnA_2O_4$ formation in the presence of LiF were observed for specimens including both coarse and dense alumina and agglomerates of fine alumina, and their morphological changes were compared with each other. LiF formed an intermediate liquid phase with ZnO and $Al_2O_3$. In the specimen with agglomerated $Al_2O_3$, the porous $ZnAl_2O_4$ layer was developed from the $Al_2O_3$ agglomerates. However, on firing at 700° C, zeta-lithium aluminate developed just inside the $ZnAl_2O_4$ layer and interfered with the spreading of the liquid including $Al_2O_3$ to the ZnO phase. However, on firing above 800° C, the formation of $ZnAl_2O_4$ was promoted by the rapid spreading of the fluoride liquid including $Al_2O_3$ to the ZnO phase through the porous $ZnAl_2O_4$ layer before $LiAl_5O_8$ formation. In the specimen with coarse and dense $Al_2O_3$, the dense $ZnAl_2O_4$ layer grew around the coarse and dense $Al_2O_3$ and the fluoride liquid phase was confined between the $ZnAl_2O_4$ layer and the $Al_2O_3$ particles. The dense $ZnAl_2O_4$ layer interrupted the spread of the liquid phase to the ZnO phase and interfered with further formation of $ZnAl_2O_4$. The confined liquid phase gradually reacted with $Al_2O_3$ to form $LiAl_5O_8$. It is necessary for the fluoride liquid including $Al_2O_3$ to spread out to the ZnO phase through the porous $ZnAl_2O_4$ layer to form $ZnAl_2O_4$, before the dense $ZnAl_2O_4$ or $LiAl_5O_8$ layer grew around $Al_2O_3$. The use of fine $Al_2O_3$ powder and a high firing temperature were effective in the promotion of $ZnAl_2O_4$ formation in the presence of LiF.

## 1. Introduction

We have reported that $ZnAl_2O_4$ formation with lithium fluoride is affected by the particle size of alumina [1], aggregates or agglomerates of alumina and compaction pressures in forming the specimen compacts [2]. LiF promoted $ZnAl_2O_4$ formation, i.e. enhanced the yield of the product and lowered the initiation temperature of the reaction. The rate curves for the specimen with LiF indicated the operation of a mechanism of $ZnAl_2O_4$ formation different from that of the system without LiF, where diffusion controlled the rate, i.e. the parabolic rate law [3–7]. Alumina of a particle size finer than $10\,\mu m$ was preferable in the promotion of $ZnAl_2O_4$ formation with LiF, because interference of $ZnAl_2O_4$ formation by the formation of a by-product ($LiAl_5O_8$) was found in specimens containing starting $Al_2O_3$ of a grain size larger than $10\,\mu m$. The amount of $ZnAl_2O_4$ decreased with increasing degree of agglomeration or aggregation when the firing temperature was low, but no effect was observed at high temperatures. Similar effects were also observed for the compaction pressures. However, owing to insufficient microstructural observation, the function of LiF on the reaction mechanism was not fully understood. Therefore, it is necessary to elucidate how processing factors promote $ZnAl_2O_4$ formation in the presence of LiF. In the reaction mix-

ture containing coarse $Al_2O_3$, fine ZnO and LiF, an intermediate liquid phase which contained LiF, $Al_2O_3$ and ZnO was found around the alumina particles by microstructural observation [8]. The formation of $ZnAl_2O_4$ was promoted by the migration of raw materials through this intermediate phase. Thus, it is confirmed that observation of microstructure is important in examining the formation of $ZnAl_2O_4$ with fluoride, because the microstructure was the result of the behaviour of reactants, products and additives.

The purpose of the present work was to investigate the effect of the physical nature of alumina on $ZnAl_2O_4$ formation with LiF, by observing the microstructural changes during the reaction. The microstructure of $ZnAl_2O_4$ formation from the system of the agglomerates of fine $Al_2O_3$ particles and ZnO was compared with that from the system of coarse $Al_2O_3$ and ZnO particles. In particular, the behaviour of an intermediate phase in those systems is observed microscopically and examined to clarify how the intermediate phase affects the microstructural changes of the $ZnAl_2O_4$ formation.

## 2. Experimental procedure
### 2.1. Materials
Alpha-alumina, of primary particle size $0.2\,\mu m$, from
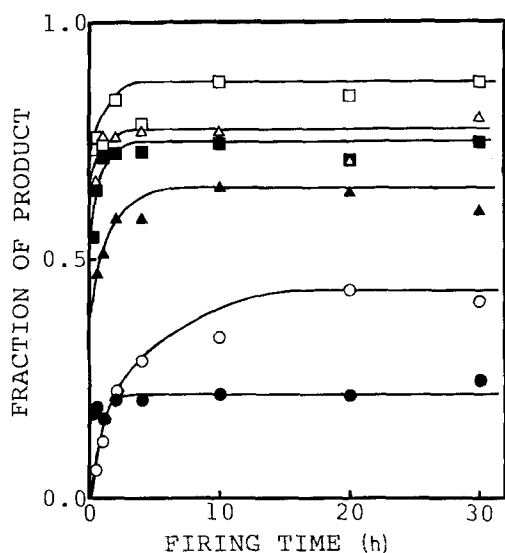
Figure 1 Rate curves of ZnAl₂O₄ formation in samples I (open symbols) and II (solid symbols) in the presence of LiF fired at various temperatures. (○, ●) 700° C, (△, ▲) 800° C, (□, ■) 900° C.



Figure 2 Relative intensity of X-ray diffraction in samples I (open symbols) and II (solid symbols) fired at the indicated temperatures. (○, ●) ZnAl₂O₄, (◇, ◆) ZnO, (□, ■) Al₂O₃, (△, ▲) LiAl₅O₈.

the Aluminium Co. of America (Alcoa A-16 SG) was used as the fine alumina material. By spray-drying of fine alumina, agglomerates of alumina of 40 μm average diameter were prepared. The starting material of coarse aluminium oxide was fused alpha-alumina (Fujimi Kenma Co., Japan), which has 98.5% purity and an average diameter of 60 μm. The source of ZnO was a GR grade of 0.3 μm average diameter from the Kishida Chemicals Co., Japan. Extra-pure lithium fluoride from the Nakarai Chemicals Co., Japan, was used.

## 2.2. Sample preparation and firing

Lithium fluoride (20 mol %) was added to an equivalent molar mixture of ZnO and Al₂O₃, to produce two samples. In sample I, the mixture including agglomerated Al₂O₃ was blended in a polyethylene bottle to avoid the breakdown of the agglomerated Al₂O₃. In sample II, the mixture including coarse Al₂O₃ was tumbled in a polyethylene bottle with 5 mm diameter glass beads. The mixture was compacted in a 10 mm diameter steel die under a uniaxial pressure of 15 MPa. The compacts were heated in an electric furnace at a temperature from 700 to 900° C for various durations in an argon atmosphere. The fluctuation of temperature was ± 5° C at each temperature. At the end of the run, the compacts were quickly cooled.

## 2.3. Phase analysis and microstructural observation

Phases in the fired specimens were identified using a conventional powder technique by X-ray diffraction (XRD) analysis (Jeol Model JDX 7E). Green and fired compacts were impregnated with epoxy resin and subjected to grinding and final polishing with 2 μm diamond paste. Polished samples were observed by optical microscopy in reflected light and also by scanning electron microscopy (SEM). The chemical constituents in the microstructure were thoroughly traced using an energy dispersive X-ray microanalyser
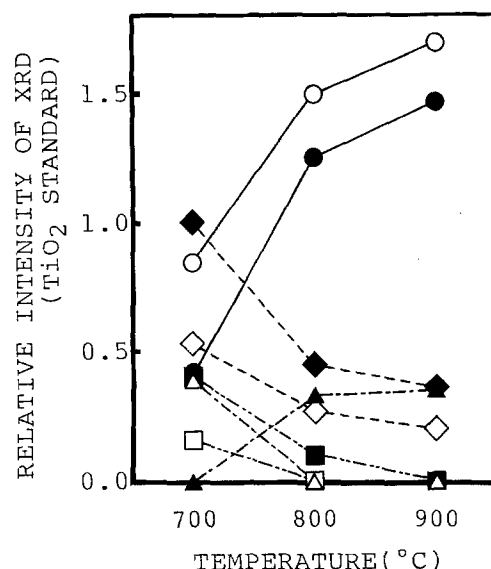
(EDX) (Horiba Ltd, model EMAX 8000 S) attached to the SEM. However, using an EDX analyser it is almost impossible to detect fluoride ions directly because of the low intensity of their X-ray emission [9]. We have developed a method of fluorine detection [10] on an EDX analyser and have applied it to the present study. The essence of this method is the exchange of the cation of fluoride in the samples for a distinguishable cation. CaCl₂ or Th(NO₃)₄ aqueous solution was mostly used for this purpose. A Hitachi Model H 800 transmission electron microscope was also employed to determine particle size of the starting powders.

## 2.4. Determination of the extent of ZnAl₂O₄ formation

The extent of ZnAl₂O₄ formation was calculated from the amount of residual ZnO. The amount of ZnO was determined chemically by dissolving ZnO with 2 mol dm⁻³ HCl solution and titrating Zn²⁺ with 0.01 mol dm⁻³ EDTA solution with EBT as the indicator at pH 10.

## 3. Results and discussion
### 3.1. Effect of LiF addition

The effects of LiF additive on the formation of ZnAl₂O₄ from samples I and II were examined. Fig. 1 shows the extent of ZnAl₂O₄ formation with firing time at various temperatures. In both samples I and II the tendency of the rate curves is similar; the amount of ZnAl₂O₄ increases up to a certain value in the early stage of the reaction and then shows a constant value at each temperature. However, the constant values in sample I are seen to be higher than those of sample II at each temperature.

As shown in Fig. 2, XRD analyses of sample II including coarse Al₂O₃ fired at a high temperature (800 and 900° C) indicate the formation of zeta-lithium aluminate (LiAl₅O₈). On the other hand, the formation of LiAl₅O₈ in sample I is limited at a low temperature (700° C).
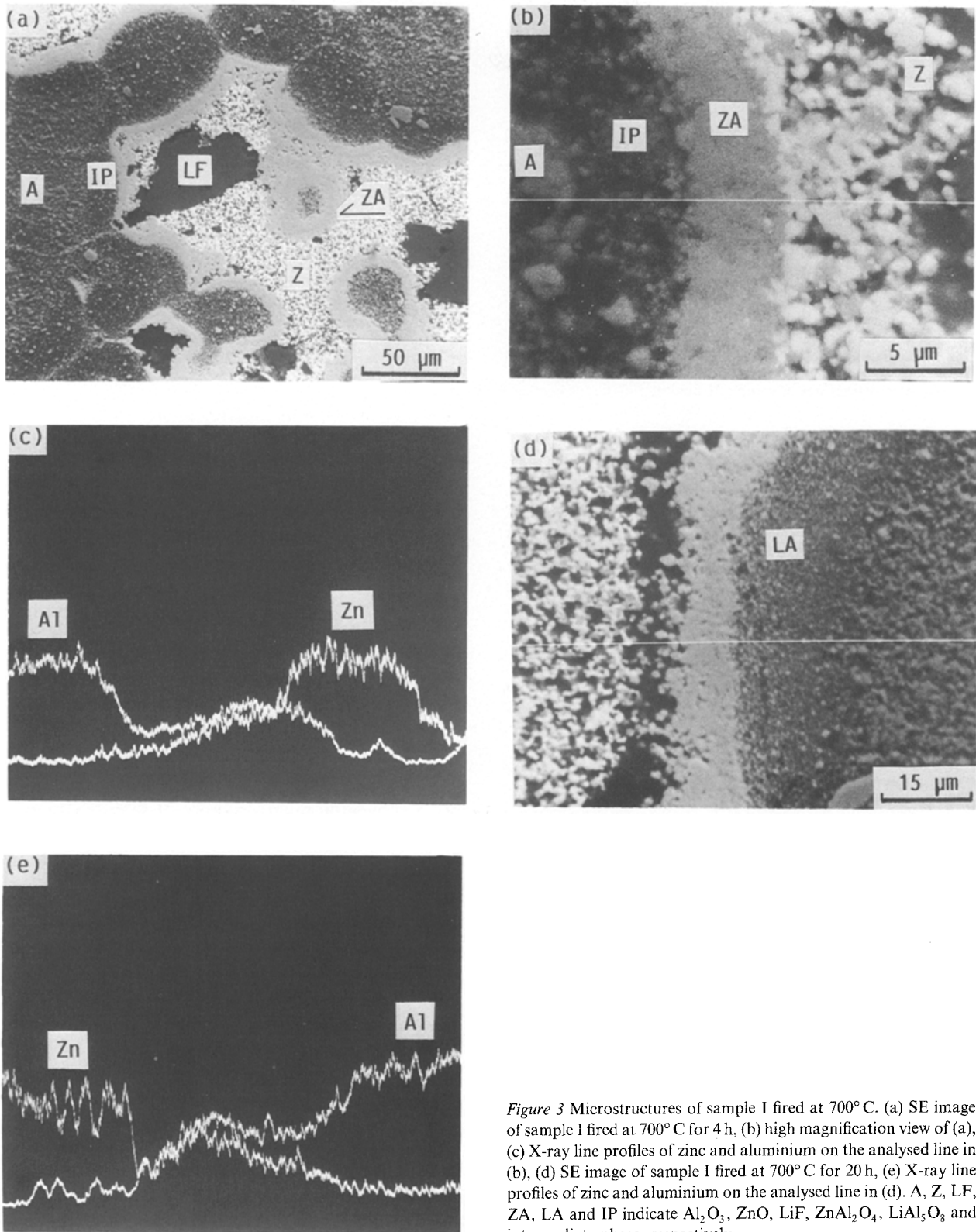
*Figure 3* Microstructures of sample I fired at 700° C. (a) SE image of sample I fired at 700° C for 4 h, (b) high magnification view of (a), (c) X-ray line profiles of zinc and aluminium on the analysed line in (b), (d) SE image of sample I fired at 700° C for 20 h, (e) X-ray line profiles of zinc and aluminium on the analysed line in (d). A, Z, LF, ZA, LA and IP indicate $Al_2O_3$, ZnO, LiF, $ZnAl_2O_4$, $LiAl_5O_8$ and intermediate phase, respectively.

## 3.2. Microstructural changes at 700° C

Representative microstructures of samples I and II fired at a low temperature are shown in Figs 3 and 4. Fig. 3 shows the micrographs and the results of EDX analyses for sample I including agglomerated $Al_2O_3$ fired at 700° C, which is close to the starting temperature of $ZnAl_2O_4$ formation; the $ZnAl_2O_4$ layer with many interspaces was produced at the alumina side of the boundary zone between zinc oxide and alumina (Figs 3a and b). LiF formed an intermediate phase

including ZnO and $Al_2O_3$ as described above. The intermediate phase is found in a darkish layer developed in the $Al_2O_3$ granule just inside the $ZnAl_2O_4$ layer. In the early stages of reaction, zinc oxide was mainly transported by diffusion through the intermediate phase into the $Al_2O_3$ phase (Fig. 3c; line profiles of $ZnK\alpha$ and $AlK\alpha$). However, after long firing times, small $ZnAl_2O_4$ particles were found in the ZnO phase (Fig. 3d): the transport of $Al_2O_3$ to the ZnO phase occurred at the same time, although its rate was

4269
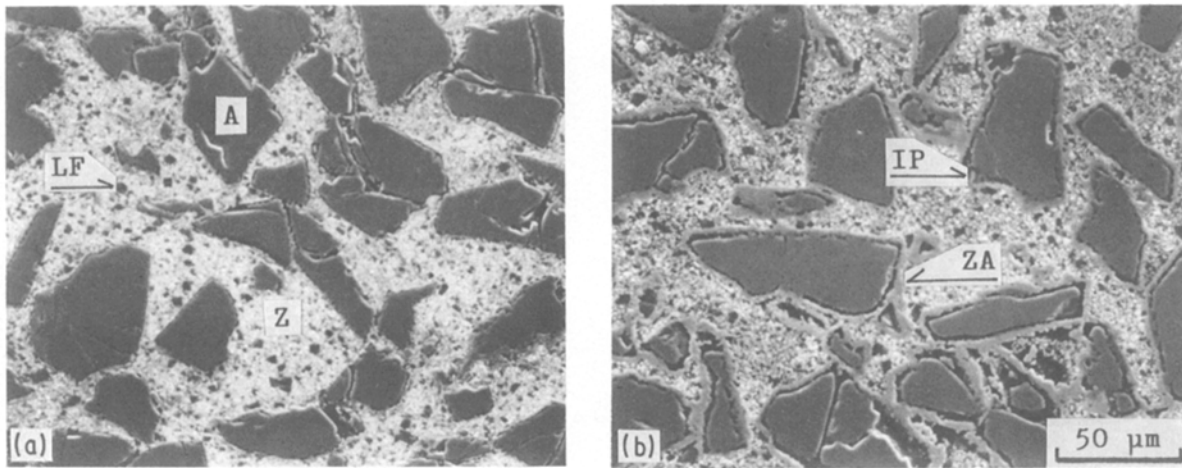
*Figure 4* Microstructures of sample II fired at 700°C, for (a) 0.25 h, (b) 20 h.

very small. After long firing times, a diffuse layer of zinc was observed in the alumina agglomerate. $LiAl_5O_8$ was confirmed in the diffuse layer of zinc in the $Al_2O_3$ phase and the intermediate phase existed in the centre of the $Al_2O_3$ granule as shown in Figs 3d and e, i.e. in spite of the penetration of the intermediate phase to the centre of the $Al_2O_3$ granule, the $ZnAl_2O_4$ layer which forms is almost restricted to the neighbourhood of the interface between the $Al_2O_3$ agglomerates and the ZnO powder. From these results, it may be suggested that the spreading rate of the intermediate phase is higher than that of the dissol-

ution rate of oxides, or of the diffusion rate of ions which resulted ion the dissolution of oxides into the intermediate phase.

Fig. 4 shows the microstructure of sample II fired at 700°C for 20 h. As seen in Fig. 4a, corrosion of $Al_2O_3$ by LiF is observed around $Al_2O_3$ particles. Fig. 4b shows that $ZnAl_2O_4$ was formed in a layer just around the $Al_2O_3$ particles, and the intermediate liquid phase was found in the interspace between the $ZnAl_2O_4$ layer and the $Al_2O_3$ particle. The $ZnAl_2O_4$ layer was developed by the migration of $Al^{3+}$ ions through the intermediate phase and by its diffusion through the $ZnAl_2O_4$ layer into the ZnO phase.
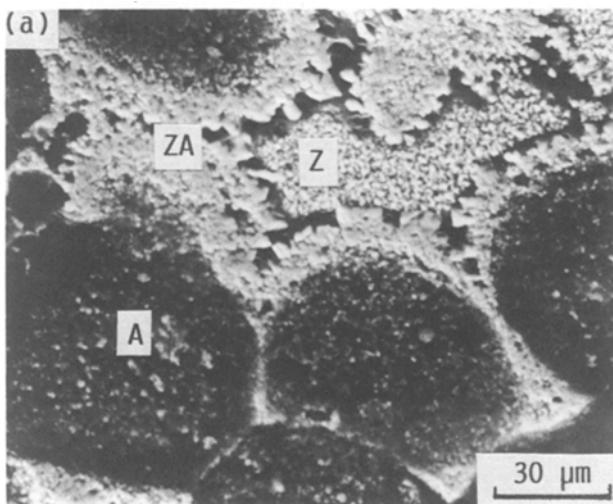
## 3.3. Microstructural changes above 800°C

Fig. 5 shows the microstructure of sample I fired at 800°C for 20 h. $ZnAl_2O_4$ was mainly observed in the ZnO phase in contrast to the case at 700°C. Many coarse $ZnAl_2O_4$ crystals were formed in the ZnO phase by transport of $Al_2O_3$. The maps of zinc and aluminium distribution at 800°C obtained by EDX analysis are shown in Figs 5b and c. They suggest that aluminium was carried by the fluoride liquid from the $Al_2O_3$ phase to the ZnO phase, whereas a small amount of zinc moved from the ZnO phase to the



*Figure 5* SEM and EDX analyses of $ZnAl_2O_4$ formation in sample I fired at 800°C for 20 h. (a) SE image, (b) X-ray image of zinc, (c) X-ray image of aluminium.
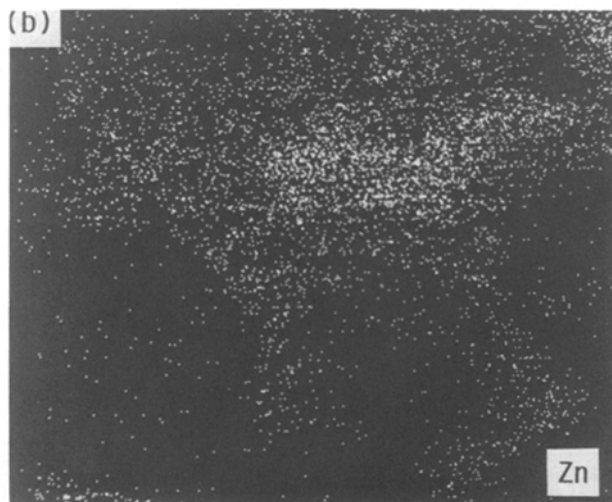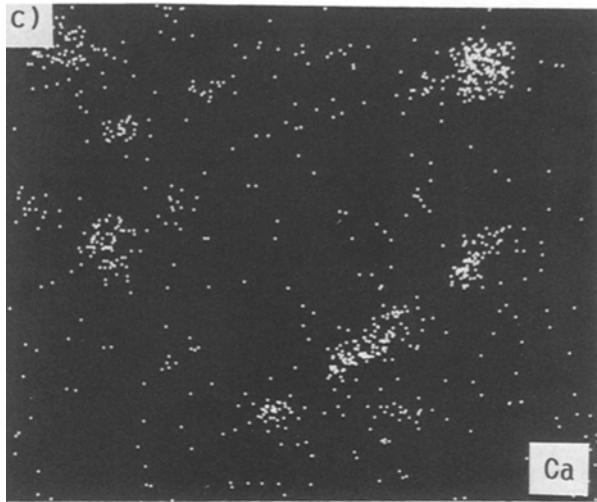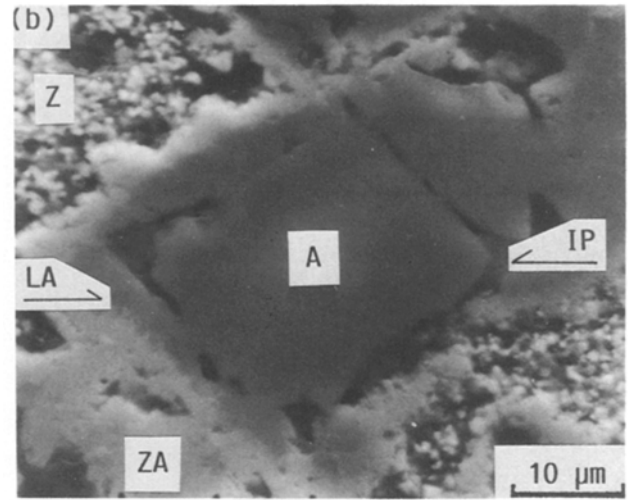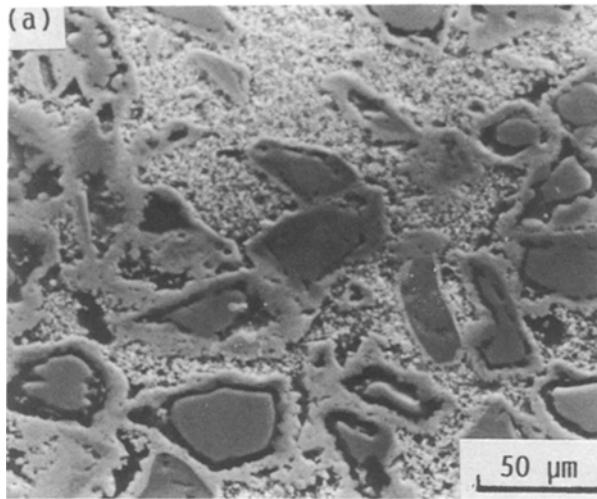
Figure 6 SEM and EDX analyses of $ZnAl_2O_4$ formation in sample II fired at 800°C for 2 h. (a) SE image, (b) high magnification view of (a), (c) X-ray image of $CaK\alpha$.

$Al_2O_3$ phase. When agglomerated $Al_2O_3$ was used as a starting material, a $ZnAl_2O_4$ layer with many interspaces was produced. Through the interspaces the fluoride liquid carries $Al_2O_3$ to the ZnO phase, and $ZnAl_2O_4$ forms in the ZnO phase without $LiAl_5O_8$.

Fig. 6 shows the microstructure of sample II fired at a high temperature and also shows the results of the fluorine detection method by EDX using $Ca^{2+}$ as a fluoride ion marker applied to this sample. Figs 6a, b
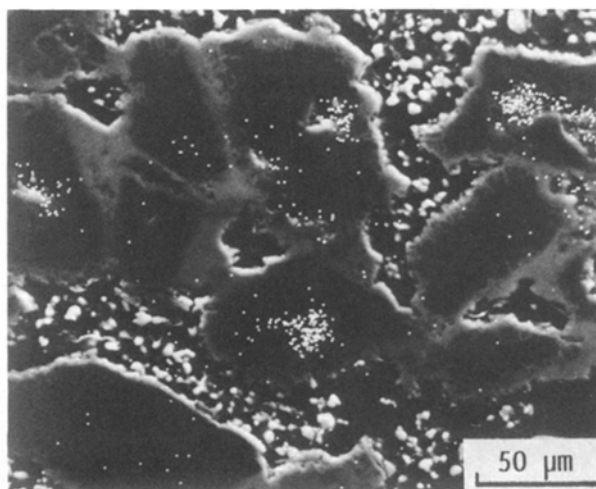


Figure 7 Microstructure of sample II in the final stage of the reaction. White dots indicate the X-ray image of $CaK\alpha$.

and c show a scanning electron image, the higher magnification view of (a) and the X-ray line profile of $CaK\alpha$ on the surface indicated in photo (b), respectively. As seen in Fig. 6a, $LiAl_5O_8$ was deposited from the intermediate liquid phase just inside the $ZnAl_2O_4$ layer. Growth of the $ZnAl_2O_4$ layer apparently ceases at this stage because transport of $Al_2O_3$ to the ZnO phase through the liquid was interrupted by the dense $ZnAl_2O_4$ layer and the $LiAl_5O_8$ layer. Calcium was found principally on the polished surface of the inter-mediate phase, indicating that fluoride ions existed in the phase as shown in Fig. 6c. This result indicates that the intermediate phase is confined between the $LiAl_5O_8$ phase and the $Al_2O_3$ phase.

Fig. 7 shows the micrograph of sample II in the final stage of reaction and also shows an X-ray map of $CaK\alpha$ by overlapping on the secondary elec-tron image. $ZnAl_2O_4$ and $LiAl_5O_8$ grew densely and formed in the double layers which interrupt the migra-tion of the intermediate liquid phase and further growth of the $ZnAl_2O_4$ layer. As seen in Fig. 7, calcium was detected in the centre of the particles, i.e. the intermediate liquid phase exists in the centre of the particles.

### 3.4. Schematic reaction model
Microstructural observation allowed a schematic reaction model to be drawn of the $ZnAl_2O_4$ formation affected by the physical nature of $Al_2O_3$ in the presence of LiF. Fig. 8 shows the schematic reaction model for the specimen with agglomerated $Al_2O_3$. It was found by microstructural observations that the reaction proceeded as follows.

(i) On firing at 700°C, LiF formed an intermediate liquid phase around the interface between $Al_2O_3$ and ZnO.

(ii) The $ZnAl_2O_4$ layer having many interspaces grew into the $Al_2O_3$ agglomerates by transport of ZnO through this liquid phase.

(iii) Zeta-lithium aluminate, $LiAl_5O_8$, formed just inside the $ZnAl_2O_4$ layer, because the intermediate

4271

Morphology          Rate curves          Morphology          Rate curves
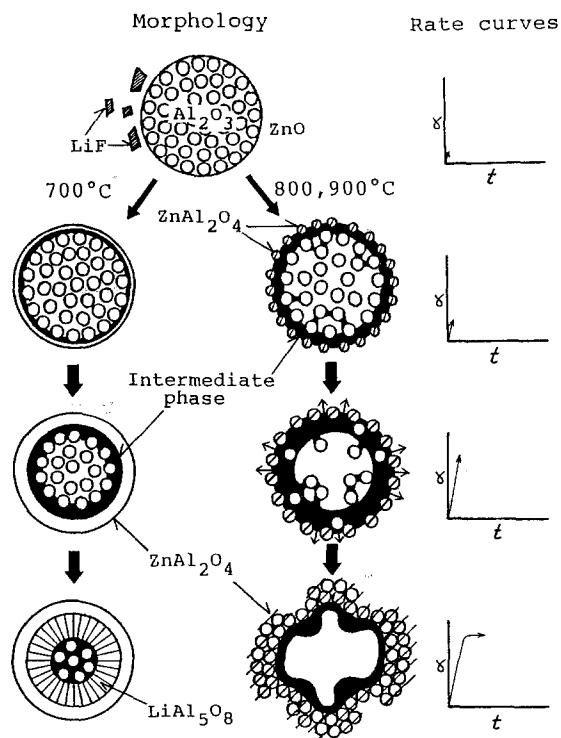


Figure 8 Schematic reaction model for sample I.



Figure 9 Schematic reaction model for sample II.

phase penetrated into the $Al_2O_3$ agglomerates and reacted with $Al_2O_3$.

However, on firing above 800° C:

(i) No formation of $LiAl_5O_8$ was found on firing above 800° C due to the rapid dissolution of $Al_2O_3$ into the intermediate liquid phase.

(ii) Coarse and dense $ZnAl_2O_4$ was formed in the ZnO phase by transport of $Al_2O_3$ through the liquid phase and the porous $ZnAl_2O_4$ layer.

Fig. 9 shows the schematic reaction model for the specimen with coarse $Al_2O_3$. Microstructural observations indicated four steps in $ZnAl_2O_4$ formation.

(i) LiF gave rise to an intermediate liquid phase around $Al_2O_3$ particles, which contained LiF, zinc and aluminium.

(ii) Dense $ZnAl_2O_4$ developed by transport of $Al^{3+}$ through the intermediate phase and by diffusion of it through the $ZnAl_2O_4$ layer.

(iii) The dense $ZnAl_2O_4$ layer interrupted the intermediate phase and spread out to the ZnO phase; the liquid fluoride phase was confined between the $ZnAl_2O_4$ layer and the $Al_2O_3$ phase. The confined intermediate liquid phase reacted with $Al_2O_3$ to form $LiAl_5O_8$.

(iv) Further dissolution of $Al_2O_3$ by the intermediate phase promoted the growth of $LiAl_5O_8$ and the migration of the liquid to the centre of the $Al_2O_3$ particles.

The use of the agglomerates of fine alumina was effective in the promotion of $ZnAl_2O_4$ formation by the formation of a porous $ZnAl_2O_4$ layer and by the spreading of the intermediate liquid phase over the whole of the sample through the porous $ZnAl_2O_4$ layer when firing was carried out at a high temperature. Consequently, if rapid dissolution of $Al_2O_3$ into the

intermediate liquid phase occurs and the liquid can easily spread over the whole of the specimen before the dense $ZnAl_2O_4$ wall starts to grow around the $Al_2O_3$ particles, $ZnAl_2O_4$ formation is maximized. If the dense $ZnAl_2O_4$ wall is formed first, the permeation of $Zn^{2+}$ and/or $Al^{3+}$ into the liquid is prevented and no further $ZnAl_2O_4$ is formed, and $LiAl_5O_8$ becomes saturated instead.

## References

1.  M. HASHIBA, Y. NURISHI and T. HIBINO, J. Mater. Sci. in press.
2.  Idem, ibid.
3.  D. L. BRANSON, J. Amer. Ceram. Soc. 48 (1965) 591.
4.  M. R. ANSEAU, F. CAMBIER and C. LEBLUD, J. Mater. Sci. 16 (1981) 1121.
5.  H. KAWAKAMI, H. OKADA, M. HASHIBA, E. MIURA, Y. NURISHI and T. HIBINO, Yogyo Koyokai-Shi 90 (1982) 648.
6.  Y. HUKUHARA, E. SUZUKI, M. HASHIBA, E. MIURA, Y. NURISHI and T. HIBINO, ibid. 91 (1983) 281.
7.  H. OKADA, H. KAWAKAMI, M. HASHIBA, E. MIURA, Y. NURISHI and T. HIBINO, J. Amer. Ceram. Soc. 68 (1985) 58.
8.  M. HASHIBA, E. MIURA, Y. NURISHI and T. HIBINO, Nippon Kagakukai-Shi. 1983 (1983) 501.
9.  J. I. GOLDSTEIN, D. E. NEWBURY, P. ECHLIN, D. C. JOY, C. FRIORI and E. LIFSHIN, "Scanning Electron Microscopy and X-Ray Microanalysis" (Plenum, New York, 1981) p. 263.
10.  M. HASHIBA and Y. NURISHI, unpublished data.